A Scenario Generation Method for Wind Power Ramp Events Forecasting

Mingjian Cui, *Student Member, IEEE*, Deping Ke, Yuanzhang Sun, *Senior Member, IEEE*, Di Gan, Jie Zhang, *Member, IEEE*, and Bri-Mathias Hodge, *Member, IEEE*

***Abstract*—Wind power ramp events (WPREs) have received increasing attention in recent years due to their significant impact on the reliability of power grid operations. In this paper, a novel WPRE forecasting method is proposed which is able to estimate the probability distributions of three important properties of the WPREs. To do so, a neural network (NN) is first proposed to model the wind power generation (WPG) as a stochastic process so that a number of scenarios of the future WPG can be generated (or predicted). Each possible scenario of the future WPG generated in this manner contains the ramping information, and the distributions of the designated WPRE properties can be stochastically derived based on the possible scenarios. Actual data from a wind power plant in the Bonneville Power Administration (BPA) was selected for testing the proposed ramp forecasting method. Results showed that the proposed method effectively forecasted the probability of ramp events.**

***Index Terms*—Genetic algorithm (GA), neural networks, stochastic process model, stochastic scenario generation, wind power ramp events, ramp forecasting**

I. Introduction

The integration of large amounts of wind power, which has variable and uncertain power output, poses challenges in maintaining the power system's traditional levels of reliability [1]. Large fluctuations of wind power in a short time period, such as significant increases or decreases, are known as wind power ramp events (WPREs) [2]-[4]. WPREs are particularly important in the management and dispatch of wind power. It is sometimes necessary to regulate the output of traditional generators in the power grid to accommodate the substantial fluctuations of wind power, including using grid ancillary services or curtailing the wind turbine output. These actions can have significant economic impacts, and so better forecasting of these events could mitigate the effects; research on WPREs forecasting has shown how this can benefit system operations [5]. Better forecasting of WPREs helps the power system operator, especially at the economic dispatch timescale.

Sevilian and Rajagoapal [6] defined a family of scoring functions with ramp events definitions and used a dynamic programming recursion technique to detect all the ramp events. Cutler et al. [7] forecasted ramp events and evaluated the efficiency of the Wind Power Prediction Tool (WPPT) and the Mesoscale Limited Area Prediction System (MesoLAPS) for ramp events forecasting. Ramp events in [8] were grouped in classes and the SVM method was used to forecast and classify ramp events. Bossavy et al. [9] used the ramp durations and ramp intensity of the predicted ramp events as additional variables to improve the reliabilities of quantiles forecasting. It mapped a number of ensemble members forecasting a specific ramp event to a probability of that ramp actually occurring, and produced confidence intervals of ramps occurring.

The organization of this paper is as follow. In Section II, a stochastic scenario generation method is briefly developed. In Section III, the neural network (NN) based stochastic process model is presented. The experimental results are described in Section IV. Section V concludes the paper.

II. The Stochastic Scenario Generation Method

Compared to most of the conventional approaches, which commonly predict the values of WPG, the method proposed in this paper essentially outputs the occurrence probabilities of all possible values of future WPG. Specifically, it relies on a novel stochastic process model (Fig. 1(a)) which calculates the probabilities based on the available WPG data. WPG is uniformly discretized to M discrete values denoted by u_i (i=1, 2,…, M) over the range of [0, P_{wmax}], where P_{wmax} is the maximum wind power output of the wind plant. At any instant in time, the WPG data (measured or predicted) should be among these M possible values. The discretization can accurately reflect the continuous data case if M is selected to be sufficiently large. Moreover, X_t is used to represent the existing WPG data at the current time instant t while the predicted WPG data at the future time instant t+1 is expressed by $\bar{X}_{t+1}$. Therefore, at the time instant t, the inputs of the model (shown in Fig. 1(a)) are the m consecutive WPG data from the time instant t-m+1 to t and a possible value of WPG at the time instant t+1. The output of the model is the occurrence probability ($p_{i,t+1}$) of the WPG. A large number of scenarios are generated as a scenario pool, which is introduced in Section B. All M possible values of WPG are utilized as the m+1 input to the model (with the other inputs fixed) at the time instant t, and their occurrence probabilities at the time instant t+1 are calculated. Then the cumulative density function (CDF) of $\bar{X}_{t+1}$ can be derived by cumulating these probability values along with u_1, u_2,…, u_M in an ascending order. Such process is schematically depicted in Fig. 1(b).

M. J. Cui, Y. Z. Sun, D. P. Ke and D. Gan are with the School of Electrical Engineering, Wuhan University, Wuhan 430072 China (e-mail: mj_cui@whu.edu.cn; yzsun@mail.tsinghua.edu.cn; ee-dp.ke@connect.polyu.hk; hubeigandi@whu.edu.cn).

J. Zhang and B. M. Hodge are with National Renewable Energy Laboratory (NREL), Golden, CO 80401, USA (e-mail: {jie.zhang, bri.mathias.hodge}@nrel.gov).

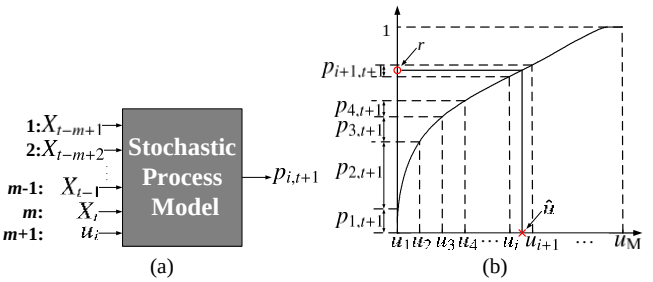

Fig. 1. (a) A novel stochastic process model; (b) Schematic diagram for deriving CDF with probability values.

Therefore, in order to entirely mimic the phenomena in the stochastic environment, more meaningful manipulations to produce $\bar{X}_{t+1}$ are proposed as follows: (i) first, randomly generate a uniformly distributed variable *r* from the Uniform distribution over [0, 1] [10]; (ii) second, from that point draw a horizontal line to intersect with the CDF curve; and (iii) finally, project the intersection point to the horizontal axis to get a point ($\hat{u}$) identified by a cross, and if $u_i < \hat{u} \le u_{i+1}$, then $\bar{X}_{t+1} = u_{i+1}$. These operations are termed in this paper as the random trial based realization.

A. Scenario Pool Generation

By using the random trial based realization, the proposed stochastic process model can be further utilized to predict several subsequent steps' WPG data from the current time (e.g. $\bar{X}_{t+1}$, $\bar{X}_{t+2}$, $\bar{X}_{t+3}$, …, $\bar{X}_{t+\mathrm{L}}$). Once $\bar{X}_{t+1}$ is generated, it replaces X_t as the *m* input of the model shown in Fig. 1(a). X_t replaces X_{t-1} as the *m*-1 input while X_{t-1} replaces X_{t-2} as the *m*-2 input. Such replacements continue propagating until X_{t-m+1} as the 1st input. Then, by keeping these *m* inputs fixed and setting the *m*+1 input to be u_1, u_2, …, u_M, respectively, the CDF of the WPG at the time instant *t*+2 is constructed as described in the previous subsection. With this CDF, $\bar{X}_{t+2}$ is obtained via the random trial based realization. Similarly, $\bar{X}_{t+3}$ to $\bar{X}_{t+\mathrm{L}}$ are sequentially calculated by repeating the above manipulations in a recursive manner.

The random number *r* (uniformly distributed) must be regenerated during each random trial to produce a scenario. Therefore, if this scenario generation procedure is repeated $\mathrm{N_s}$ times at the current time instant, $\mathrm{N_s}$ scenarios will be produced. These scenarios compose a scenarios pool at the current time instant, and each of them describes one possible WPG evolving trajectory in the future (limited to L steps). From the respect of sampling analysis, the scenarios pool could be regarded as a Monte Carlo simulation of the stochastic process if $\mathrm{N_s}$ is selected to be adequately large, and it naturally covers the stochastic characteristics contained in the process model.

The credibility of the scenarios pool and the ramping information extracted from the scenarios (Section IV) greatly depends on the quality of the stochastic process model. Thus, a novel NN-based stochastic process model is constructed and trained based on the historical WPG data, which is introduced in the subsequent section.

III. NN-Based Stochastic Process Model

A three-layer feed-forward NN is employed to develop the stochastic process model, due to its generality and capability of approximating nonlinear functions [11]. The sigmoidal function is designated as the activation function while the linear function is used as the output function.

A. Objective Function for Training

It is expected that the WPG data series (the scenario) generated by the NN (the stochastic process model) can fully fit the probabilistic characteristics of the measured stochastic process. To achieve this, this study considers two probabilistic characteristics which are described as follows.

1) CDF over the infinite time horizon

The CDF is fixed since it is defined with an infinite time horizon. In general, the WPG data must cover a long enough time horizon to approximate the CDF. Thus, a CDF denoted by $F_1(u)$ is constructed through the historical WPG data with a length of $\mathrm{N_h}$ coming from the measured stochastic process. Here, In the same manner, $F_2(u)$ representing another CDF is derived from the WPG data series (scenario) generated by the NN model. The length L of the scenario used here should also be large enough to encompass sufficient information of the WPG probability distribution over the infinite time horizon. Thus the necessary condition that the NN-based stochastic process model is a sufficient mathematical representation of the measured stochastic process with $F_1(u)$ and $F_2(u)$ as identical as possible, should hold. Accordingly, the following function is defined to identify the distinction between the NN model and the measured stochastic model from the aspect of the CDF over the infinite time horizon:

$$F = \sum_{i=1}^{\mathrm{M}} [F_1(u_i) - F_2(u_i)]^2 \tag{1}$$

2) Second-order autocorrelation function

The CDF mentioned above depicts the overall occurrence frequencies of the WPG values over the infinite time horizon. However, this CDF does not respect the ordinal relationships of the WPG data along the time sequence. When employing the stochastic process model, the occurrence probability of a WPG value at a certain time instant relies on several WPG data occurring in the previous time steps. This definitely manifests the relationship between the fore-and-aft data of the WPG data series. Normally, the sequential relationship of the data series is quantitatively measured in statistics by the second-order autocorrelation function (ACF) [12], [13]. Therefore, with the historical WPG data a second order ACF $C_1(\tau)$ is formed to indicate the autocorrelation property of the data. Meanwhile, the scenario (WPG data series) used to generate the CDF in the previous subsection will produce another second-order ACF $C_2(\tau)$. Thus, the error function defined in the following can intrinsically distinguish the NN model from the measured stochastic process model:

$$C = \sum_{\tau=-\mathrm{N}_\tau}^{\mathrm{N}_\tau} [C_1(\tau) - C_2(\tau)]^2 \tag{2}$$

where N_τ represents the maximum time lag considered in the

construction of the ACFs.

So far, two important probabilistic characteristics (the CDF and the ACF) have been highlighted. In order to train the NN-based stochastic process model to match the measured WPG stochastic process, the objective function for training is defined as follows:

$$f_{\text{obj}} = \mathrm{W}_1 C + \mathrm{W}_2 F \tag{3}$$

where W_1 and W_2 are the weights of the two error functions. The training process for the NN is to minimize f_{obj} so that $F_2(u)$ and $C_2(\tau)$ can fit $F_1(u)$ and $C_1(\tau)$, respectively.

The genetic algorithm (GA) is employed in this paper for the training. The individual in the population of the GA is the weights vector to be optimized, and the GA follows the standard implementation procedure which is not presented due to space limitations. During each iteration (generation), the key is to evaluate the objective function for each individual which ranks its quality among the population.

B. Validation of the NN-based Stochastic Process Model

A method is proposed to validate the NN based stochastic process model. Y_t is used to denote the data at the instant t in the verification data series. With Y_t, Y_{t+1}, …, $Y_{t+\mathrm{n}}$, the CDF of the WPG at the instant t+n+1 can be constructed according to the method in Section II.A, and it is represented by $F_{\text{ins},t+\mathrm{n}+1}(u)$. Given a confidence level η ($0 < \eta \le 1$), the corresponding quantile is obtained by taking the inverse function of $F_{\text{ins},t+\mathrm{n}+1}(u)$ as follows:

$$u_{t+\mathrm{n}+1}^{(\eta)} = F_{\text{inst},t+\mathrm{n}+1}^{-1}(\eta) \tag{4}$$

In other words, the WPG data at the instant t+n+1 should be randomly located within the confidence interval $[0, u_{t+\mathrm{n}+1}^{(\eta)}]$ with the confidence level η. It is noted that the inputs (Y_t, Y_{t+1}, …, $Y_{t+\mathrm{n}}$) to the NN model at any instant t are the real WPG data, which means that the CDF of the WPG constructed at any instant is a deterministic function. Generating the WPG data according to the CDF at any instant via the random trial based realization should be mutually independent. By setting t=1, 2, …, $\mathrm{N_v}$ respectively, $\mathrm{N_v}$ sets of WPG data will be generated. Thus, as long as the number of the data points ($\mathrm{N_v}$) is large enough, the probability of the points being located within their corresponding confidence intervals is η.

In the light of the above analysis, a flag variable $s_{t+\mathrm{n}+1}^{(\eta)}$ is defined to indicate whether the measured WPG data $Y_{t+\mathrm{n}+1}$ at the instant t+n+1 is covered by the confidence interval or not, by comparing it with $u_{t+\mathrm{n}+1}^{(\eta)}$:

$$s_{t+\mathrm{n}+1}^{(\eta)} = \begin{cases} 1 & if\ Y_{t+\mathrm{n}+1} \le u_{t+\mathrm{n}+1}^{(\eta)} \\ 0 & if\ Y_{t+\mathrm{n}+1} > u_{t+\mathrm{n}+1}^{(\eta)} \end{cases} \tag{5}$$

As t varies from 1 to $\mathrm{N_v}$, $\mathrm{N_c}$ is the number of instances where the measured WPG data reside within the confidence interval associated with η.

$$\mathrm{N_c} = \sum_{t=1}^{\mathrm{N_v}} s_{t+\mathrm{n}+1}^{(\eta)} \tag{6}$$

Therefore, if the NN model is a feasible approximation of the measured stochastic process, the number $\mathrm{N_c}/\mathrm{N_v}$ should be close to η. To ensure the adequacy of the verification, the comparisons between $\mathrm{N_c}/\mathrm{N_v}$ and η are conducted with different η values.

IV. Experimental Results

The WPG data used in this paper is from the Bonneville Power Administration (BPA). The data are sampled every 15 minutes from January 1st 2005 to December 31st 2006 and is used as the training data of the NN model. Specifically, the weights in the objective function Eq. (3) are chosen to be $\mathrm{W_1}$=$\mathrm{W_2}$=1. All calculations in this section are performed on a desktop with an Intel i7-2640M CPU @ 2.80 GHz and with 3 GB RAM.

A. Training Results and Verification

It takes around 16 hours (672 generations) for the GA to decrease the objective function to a value smaller than the specified tolerance. However, this computational time could be dramatically reduced with parallel computing. In addition, the training does not need to be run for every hour, or even every day. It can be adaptively updated monthly, seasonally, or annually in order to capture the most recent WPG data and to improve model performance.

The evolutions of the CDF and the ACF related to the NN-based stochastic process model during the training phases are shown in Fig. 2. It is seen that the GA optimization can effectively drive CDF and ACF to gradually approach their counterparts derived from the historical WPG data. Moreover, the fitting of these two functions is quite accurate when the NN model uses the final optimized weighting coefficients. This implies that the NN model can precisely mimic the measured stochastic process, at least in the sense of a consistent CDF and ACF.

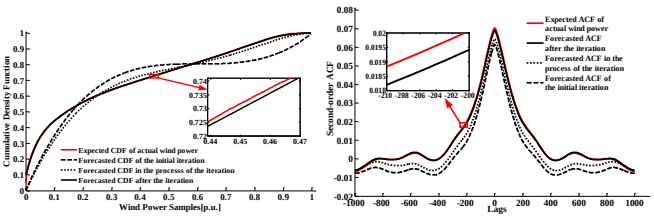

(a) CDF iterative schemes (b) ACF iterative schemes

Fig. 2. Iterative schemes of the CDF and second-order ACF.

According to the method proposed in Section III.D, given a value of η, the corresponding $\mathrm{N_c}/\mathrm{N_v}$ can be calculated from the WPG data series (scenario) generated by the NN model. The parameter $\mathrm{N_v}$ is the number of data points, and $\mathrm{N_c}$ is the number of instances where the measured WPG data reside within the confidence interval associated with η. Different $\mathrm{N_c}/\mathrm{N_v}$ ratios can be derived with multiple η values. The corresponding points (η, $\mathrm{N_c}/\mathrm{N_v}$) are plotted in Fig. 3(a) to visually show the relationship between $\mathrm{N_c}/\mathrm{N_v}$ and η. The parameter $\mathrm{N_c}/\mathrm{N_v}$ is calculated based on the NN model (identified by the circles). For the ideal case, the NN model would be an exact representation of the measured stochastic process. If the length of the historical WPG data used for the verifica-

tion is infinitely large, N_c/N_v would be strictly equal to η ($N_c/N_v=\eta$), which is represented by the blue line in Fig. 3(a).

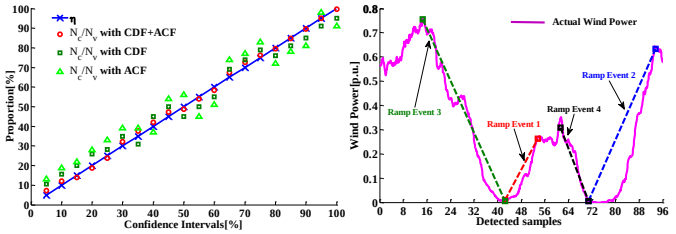

(a) (b)

Fig. 3. (a) Statistical results of η and N_c/N_v; (b) Detected actual WPREs during a certain period.

In Fig. 3(a), the circles are found to closely locate around the blue line (representing the ideal case), illustrating the accuracy of the NN-based stochastic process. Moreover, the errors between the percentage of N_c/N_v and the confidence interval associated with η can be seen by visual inspection: the red circles (by both CDF and ACF) are closer around the blue line than the dark green rectangles (only by CDF) and the green triangles (only by ACF).

B. Distribution of Single Characteristic Experiment

Detected ramp events based on the scenarios pool introduced in Fig. 3(b) are taken as the reference case, and the length of each scenario is set to be 96 time points (one day). The detecting algorithm proposed in [14] is used to identify all of the ramp events (ramp-ups and ramp-downs) and characteristics. In Fig. 3(b), there are four ramp events identified by the detecting algorithm. The specific features of these WPREs are listed in TABLE I. Statistical analysis is conducted with a large amount of forecasted characteristics data. The NN model weights are compared with different objective functions: (i) the single CDF; (ii) the single ACF; and (iii) the combination CDF and ACF. Statistical results of three ramp events features (ramp start time, ramp duration, and ramp swing) are shown in Fig. 4.

TABLE I
SPECIFIC FEATURES OF THE FOUR RAMP EVENTS

Ramp Events	Start Time [point | min]	Duration [point | min]	Swing [p.u.]
Event 1	43th | 645	11 | 165	0.2625
Event 2	71th | 1065	23 | 345	0.628
Event 3	15th | 225	28 | 420	0.7305
Event 4	61th | 915	10 | 150	0.3035

Fig. 4 illustrates that the proposed method using the combined objective function (CDF+ACF) is more accurate than the other two methods only using the CDF or the ACF objective function. This is because the CDF+ACF objective function considers not only the wind power distribution characteristics of historical wind power data but also the autocorrelation of the sequence. The reason that second-order features are more important is that each characteristic of ramp events is closely related to the temporality of actual wind power data. During the iterative process of forecasting output data, second-order features can make sorting features of output data fully conform to that of actual wind power data and guarantee the strong correlations between them. It is seen that probability density estimation calculated based on the CDF+ACF objective is more peaked, which means that statistical results of the CDF+ACF objective functions are more concentrated and have more statistical significance.

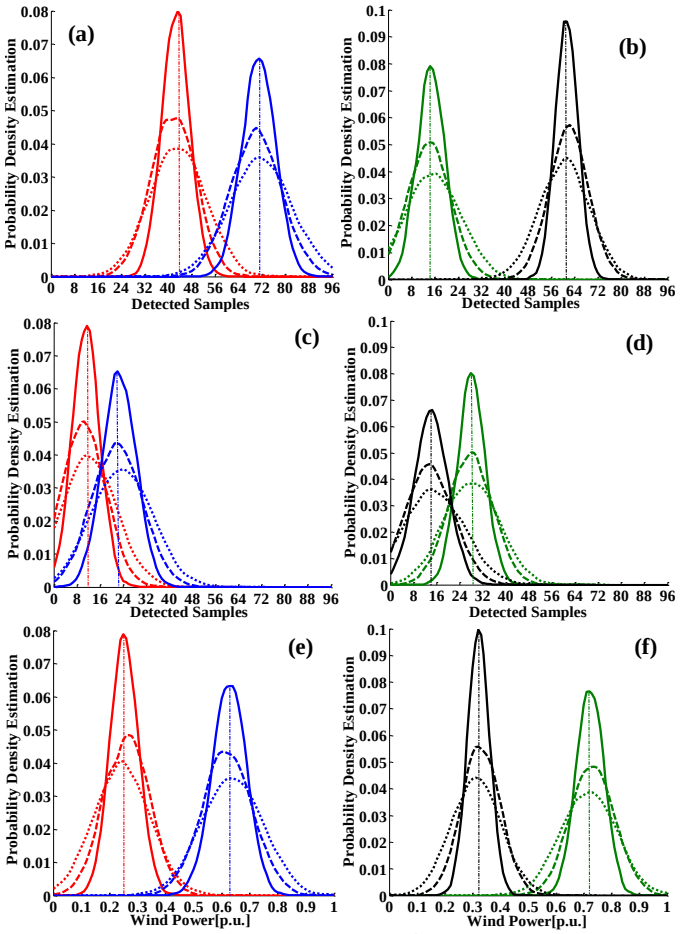

Fig. 4. Probability density estimation charts of the characteristics. Solid lines, dashed lines, and dotted lines represent using the CDF+ACF, CDF, and second-order ACF objective functions, respectively. The red line is ramp Event 1. The blue line is ramp Event 2. The green line is ramp Event 3. The black line is ramp Event 4. Figs. (a), (c), and (e) are the three estimated ramp event features (i.e. start time, duration, and swing) for ramp-ups. Figs. (b), (d), and (f) are the features for ramp-downs.

C. Utilizing Forecasted Ramp Events Statistics in Power System Analysis

After generating all the predicted scenarios (10,000 scenarios of the next whole day each with 1,440 minutes), it should be considered how to make this information more practically useful for the power system operators (PSOs), especially with high penetrations of wind power. It is important for PSOs to know when to limit the ramp rate of wind turbines and coordinate the ramp rate of the power system. Thus, all the start times of ramp events detected by using the 'L1-Trending with Sliding Window' algorithm [6], [14] and the corresponding probabilities are shown in Fig. 5. Fig. 5 illustrates four maximum probabilities at 210min, 520min, 990min, and 1110min, respectively, which require PSOs to pay more attention to these time points than other time points.

PSOs also need to decide the rates of wind power ramp

events which should be tolerated and the traditional units (especially the thermal-power units and hydro-power units) that can provide compensating power. Therefore, all the ramp events occurring at different time of the day and their values with the corresponding probabilities are depicted in Fig. 6.

The proposed probabilistic ramp forecasting method can also be used in unit commitment and economic dispatch with specific forecasting information described in TABLE II. For example, TABLE II illustrates that there is a 43.67% chance of a down ramp (with a negative value 0.009 p.u./min) at the 4th hour (in bold). This information (the maximum probability $\mathbf{P_{max}}$ and the ramp rate $\mathbf{R_v}$) can be utilized in the unit commitment.

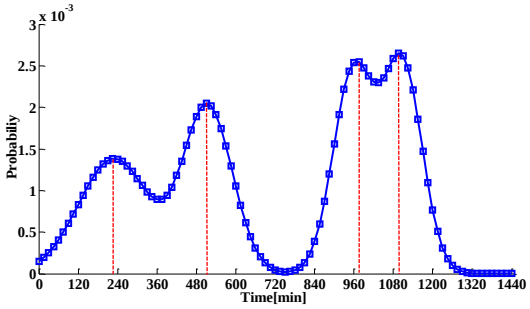

Fig. 5. Distribution of all the start times in next day (one day).

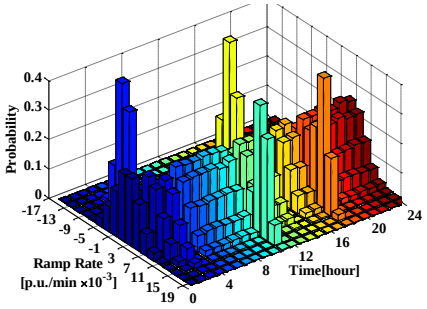

Fig. 6. Probabilities of ramp rates in the next 24 hours (one day).

TABLE II
FOUR RAMP RATES (IN BOLD) WITH EXTREMELY HIGH PROBABILITIES IN THE NEXT 24 HOURS

Time [hour]	Value [p.u./min]	Probability [%]	Time [hour]	Value [p.u./min]	Probability [%]
1	0.001	22.91	13	0.002	22.08
2	0.003	24.08	14	-0.003	23.18
3	0.005	23.33	**15**	**-0.007**	**46.30**
4	**-0.009**	**43.67**	16	0.001	22.34
5	0.003	22.90	17	0.003	24.09
6	-0.003	23.38	**18**	**0.011**	**45.37**
7	0.002	21.36	19	-0.002	23.47
8	-0.001	23.94	20	0.003	21.46
9	0.003	22.68	21	0.001	24.12
10	-0.002	23.15	22	0.002	22.96
11	**0.011**	**44.41**	23	-0.003	24.52
12	0.003	23.27	24	0.001	22.43

V. CONCLUSION

A probabilistic WPREs forecasting method was proposed in this paper. First, an NN model was developed to generate possible WPG future scenarios, which effectively approximated the measured WPG stochastic process. In particular, employing the CDF and ACF based objective function to train the NN significantly improved the accuracy of the approximation process. Moreover, a scenario pool was generated via a random trial based realization. Subsequently, the focused properties of the WPREs were extracted from each scenario and their probabilistic distributions were stochastically derived. Comparisons carried out based on real wind power data have shown that the proposed NN model could quite satisfactorily simulate the measured WPG stochastic process.

In the future work, more physical features of wind power will be considered into this model as input variables to further performance improvement, such as wind speed, wind direction, air density, and temperature.

ACKNOWLEDGE

This work was supported by the National Basic Research Program of China (2012CB215101).

REFERENCES

[1] P. Sorensen, N. A. Cutululis, A. Vigueras-Rodriguez, L. E. Jensen, J. Hjerrild, M. H. Donovan, and H. Madsen, "Power fluctuations from large wind farms," *IEEE Trans. Power Syst.*, vol. 22, no. 3, pp. 958-965, Aug. 2007.

[2] H. Zheng and A. Kusiak, "Prediction of wind farm power ramp rates: a data-mining approach," *J. Solar Energy Eng.*, vol. 131, no. 3, pp. 031011-8, Jul. 2009.

[3] N. Navid and G. Rosenwald, "Market solutions for managing ramp flexibility with high penetration of renewable resource," *IEEE Trans. Sustain. Energy*, vol. 3, no. 4, pp. 784-790, Oct. 2012.

[4] AWS Truewind. AWS Truewind's final report for the Alberta forecasting pilot project. [Online]. Available: http://www.aeso.ca/downloads/Alberta_PP_Final_Rep-ort_AWST_Jun25.pdf.

[5] C. Kamath, "Understanding wind ramp events through analysis of historical data," in *Proc. Transmission and Distribution Conf. Expo.*, New Orleans, LA, USA, 2010, pp. 1-6.

[6] R. Sevlian and R. Rajagopal, "Detection and statistics of wind power ramps," *IEEE Trans. Power Syst.*, vol. 28, no. 4, pp. 3610-3620, Nov. 2013.

[7] N. Cutler, M. Kay, K. Jacka, and T. S. Nielsen, "Detecting categorizing and forecasting large ramps in wind farm power output using meteorological observations and WPPT," *Wind Energy*, vol. 10, no. 5, pp. 453-470, Sep. 2007.

[8] H. Zareipour, D. Huang, and W. Rosehart, "Wind power ramp events classification and forecasting: a data mining approach," in *Proc. 2011 IEEE Power and Energy Soc. General Meeting*, San Diego, CA, USA, 2011, pp. 1-3.

[9] A. Bossavy, R. Girard and G. Kariniotakis, "Forecasting uncertainty related to ramps of wind power production," in *Proc. European Wind Energy Conference & Exhibition (EWEC)*, Warsaw, Poland, 2010, pp. 1-9.

[10] D. Villanueva, A. Feijoo, and J. L. Pazos, "Simulation of correlated wind speed data for economic dispatch evaluation," *IEEE Trans. Sustain. Energy*, vol. 3, no. 1, pp. 142-149, Jan. 2012.

[11] G. Sideratos and N. D. Hatziargyriou, "Probabilistic wind power forecasting using radial basis function neural networks," *IEEE Trans. Power Syst.*, vol. 27, no. 4, pp. 1788-1796, Nov. 2012.

[12] J. M. Sexauer, "Development of probabilistic load flow for voltage quality analysis in the presence of distributed generation," M.S. theis, Dept. Elect. Eng. and Computer Science, Colorado School of Mines, Golden, United States, 2012.

[13] J. F. Cardoso, "Source separation using higher order moments", in *International Conference on Acoustics, Speech, and Signal Processing*, Glasgow, Scotland, UK, 1989, pp. 2109-2112.

[14] R. Sevlian and R. Rajagopal, "Wind power ramps: detection and statistics," in *Proc. 2012 IEEE Power and Energy Soc. General Meeting*, San Diego, CA, USA, 2012, pp. 1-8.